



From useless humins by-product to Nb@graphite-like carbon catalysts highly efficient in HMF synthesis

Magdi El Fergani^a, Natalia Candu^a, Madalina Tudorache^a, Cristina Bucur^b, Nora Djelal^c, Pascal Granger^{c,*}, Simona M. Coman^{a,*}

^a Department of Organic Chemistry, Biochemistry and Catalysis, Faculty of Chemistry, University of Bucharest, Regina Elisabeta Blvd., No. 4-12, Bucharest, 030016, Romania

^b National Institute of Materials Physics, 405 Atomistilor Str., Măgurele, Ilfov, Romania

^c Univ. Lille, CNRS, Centrale Lille, ENSCL, Univ. Artois, UMR 8181 - UCCS - Unité de Catalyse et Chimie du Solide, F-59000, Lille, France

ARTICLE INFO

Keywords:

Glucose
5-hydroxymethylfurfural (HMF)
Humins valorization
Nb-based humins catalysts

ABSTRACT

Highly dispersed supported NbO_x species were prepared *via* a deposition precipitation-carbonization (DPC)-like method. As precursors for niobium species and carrier ammonium niobate(V) oxalate hydrate and humins were used. Characterization of the resulted catalysts indicated bi-functional acid-base niobium species anchored onto a highly hydrophobic graphite-like carbon structure. These catalysts were investigated in the one-pot conversion of glucose to 5-hydroxymethylfurfural (HMF) in a biphasic system consisting of a mixture of a 20 wt% NaCl aqueous solution phase and an organic extracting phase (methyl-isobutyl-ketone (MIBK), 2-tert-butylphenol (TBP) or 2-sec-butylphenol (SBP)). The optimization conditions afforded the highest yield to HMF (96 %) for the GHNb1.2 catalyst (with 2.5 wt%Nb), the base/acid sites ratio of 1.76, in biphasic TBP/water system, at 180 °C after 8 h.

1. Introduction

The environmental concerns and close associated regulations generated consistent research efforts aiming the development of new processes using biomass as a renewable source for the chemicals and energy production [1–7]. Such processes require the development of integrated conversion facilities, called biorefineries, where renewable materials are converted to compounds analogous to current oil refineries [8] in an economical, ethical and environmentally friendly way. Moreover, the complete and efficient valorization of non-edible feedstocks ensures the transition from a *linear economy* to a *circular economy* that is the key of the sustainable development.

The acid-catalyzed dehydration of carbohydrates for the production of renewable bulk chemicals, such as furfural, hydroxymethylfurfural (HMF) or levulinic acid (LA), is leading to large amounts of so-called humins (ie, carbonaceous, insoluble by-products) that are typically formed by cross-polymerization reactions of HMF and several sugar-dehydration intermediates [9–11]. Many other commercial processes based on the acid-catalyzed conversion are also seriously hampered by the extensive formation of humins by-products that leads to great losses of the feed (around 10–50 % carbon loss) and, in consequence, to

important efficiency losses in the biorefinery operations [12]. Therefore, in order to improve the efficiency of the acid-catalyzed conversion of sugars and to enhance the economic value of the process, the formation of humins should be eradicate. This is also an important challenge for the total selective synthesis of HMF or LA using both acidic homogeneous and heterogeneous catalysts [13–16]. Such an objective also requires different reaction methodologies such as aqueous/bi/multiphase organic solvent systems [17,18]. However, since the humins formation is thermodynamically favored it is quite difficult a complete elimination of these [19].

Currently, humins are used for low-value applications such as the production of energy for biorefineries [20]. However, a sustainable economy development should focus on their conversion to chemicals or to the production of functional materials but studies focusing on such applications are still scarce. Humins structure is obviously spherical consisting of a condensed, hydrophobic core and a less dense, hydrophilic shell and it depends on the synthesis conditions [20–28]. Around 60 wt% corresponds to carbon [29] in an aromatic environment consisting of essentially furanic moieties linked by ether, acetal bonds or aliphatic chains. The nature of the oxygen-containing functional groups, such as carboxyl, carbonyl, and hydroxyl and their distribution depend

* Corresponding authors.

E-mail addresses: pascal.granger@univ-lille.fr (P. Granger), simona.coman@chimie.unibuc.ro (S.M. Coman).

<https://doi.org/10.1016/j.apcata.2021.118130>

Received 29 December 2020; Received in revised form 23 February 2021; Accepted 28 March 2021

Available online 3 April 2021

0926-860X/© 2021 Elsevier B.V. All rights reserved.

on the acid catalyzed conversion of the carbohydrates process [21,22,30,31]. Despite this complexity, the humins structure recommended these as an important source of chemicals. Seshan and co-workers [20] proposed these as feedstock for hydrogen or synthesis gas production while Wang et al. [32] for the synthesis of alkyl phenolics and higher oligomers in the presence of Ru-based catalysts. Thermal pyrolysis of humins was also reported as a potential route to convert these into easily transportable fuels with a high energy density or into low molecular weight compounds from which high added value bulk chemicals, such as acetic and formic acid can be isolated [33]. To produce functional materials like composites, humins can be introduced into a polyfurfuryl alcohol network [34,35]. Other envisaged valorizations include: their utilization as functional carbon materials for soil improvement or CO₂ sequestration [36], the adsorption of metal ions, phenols [37,38] or sulfonated and even as a “green catalyst” for hydrolysis, esterification and condensation reactions [39,40]. Interestingly enough, the performances of such catalysts were superior to sulfonated amorphous glassy carbon, activated carbon or natural graphite [39,41,42]. They may also serve as support for iron oxides where demonstrated a microwave-assisted selective behavior for the oxidation of isoeugenol [43].

On the other side, the production of 5-hydroxymethylfurfural (HMF) from biomass received a special interest because it may serve as an intermediate for a large number of value added chemicals. For instance, HMF could replace terephthalic acid (TA) for the production of polyesters after the oxidation to 2,5-furandicarboxylic acid (FDCA) or it can be converted into 2,5-dimethylfuran (DMF) as a liquid biofuel [44]. The transformation of glucose to HMF is a two steps process which involves the isomerisation of glucose to fructose and the subsequent dehydration of fructose to HMF. This process requires the concerted participation of both the Lewis acid, for glucose isomerization to fructose, and Brønsted acid sites, for fructose dehydration to HMF. In this respect, dealuminated zeolites [45] and heteroatomic inserted Lewis acid, as bifunctional zeolites [18] with an improved stability in hot water, emerged as effective catalysts for the direct transformation of glucose to HMF.

Niobium compounds are highly stable in water and display remarkable catalytic acid properties as either bulk or component of the catalysts. Bulk niobia was shown to be active for the dehydration of glucose to HMF in the aqueous phase with a HMF yield of 20 % [46]. However, highly dispersed Nb species into a zeolite matrix [47] display a higher catalytic efficiency in glucose dehydration to HMF in a biphasic water/MIBK solvent [18] leading at 180 °C and after 12 h to selectivities to HMF of 84.3 % for a conversion of glucose of 97.4 %. With smaller yields (< 40 %) the isomerisation of glucose to fructose can also be catalyzed by bases [48–50]. Accordingly, solid catalysts with combined Brønsted acid and base sites emerged as efficient materials for the direct dehydration of glucose to HMF [15,51].

Carbon-loaded oxide composites demonstrated enhanced hydrothermal stability [52]. Moreover, in the particular case of the biphasic systems, carbon-loaded oxide composites are located in one of the phases, as a function of their hydrophobic/hydrophilic character, controlling in this way the catalyst's performance [53].

Herein humins by-product obtained from the dehydration of glucose was employed as carrier to prepare a niobium-based carbonaceous solid catalyst. The preparation methodology may induce structural modifications of the humins carrier with the formation of highly hydrophobic graphite-like carbon structure and acid-base functionalities. The catalytic performances of these humins-derived Nb-based catalysts were investigated in the direct dehydration reaction of glucose to HMF.

2. Experimental section

2.1. Catalysts synthesis

2.1.1. Humins

Humins (GH) were prepared by heating an aqueous solution containing D-glucose (1.0 M) and H₂SO₄ (0.01 M) in a steel autoclave at 200 °C for 12 h. The obtained humins were then isolated by filtration, washed with water, dried for 12 h at 80 °C, and grounded. After an additional Soxhlet extraction with water for 24 h, the samples were dried for 24 h at 80 °C. Following the described preparation conditions, humins were obtained with an yield of 30 %.

2.1.2. Niobium deposition

Catalysts with 1.2 (0.03 mol%, 2.5 wt%) (GHNb1.2) and 1.7 mmols Nb (0.04 mol%, 3.5 wt%) (GHNb1.7) were prepared by a deposition precipitation-carbonization (DPC) method reported in literature [52,53] adapted for the use of humins, as following: urea (CON₂H₄, 0.3 g) and ammonium niobate(V) oxalate hydrate (C₄H₄NNbO₉xH₂O, 0.36 or 0.51 g) were added to a slurry of 4.0 g of humins in 250 mL dionized water. The mixture was heated in an autoclave at 200 °C for 12 h. The separated solid was then calcined at 450 °C, for 4 h, in a N₂ flow of 30 cm³ min⁻¹.

2.2. Catalysts characterization

The resulted catalysts were exhaustively characterized by: X-ray diffraction (XRD), dynamic light scattering (DLS), thermogravimetric-differential thermal analysis (TG-DTA), IR diffuse reflectance spectroscopy with Fourier transform (DRIFT), NH₃- and CO₂-temperature programmed desorption (NH₃-, CO₂-TPD), X-ray photoelectron spectroscopy (XPS) and Scanning Electron Microscopy (SEM) coupled with Energy-dispersive X-ray spectroscopy (EDX) for elemental analysis.

Powder XRD patterns were collected at room temperature using a Shimadzu XRD-7000 apparatus with the Cu K α monochromatic radiation of 1.5406 Å, 40 kV, 40 mA at a scanning rate of 0.1 2 θ min⁻¹, in the 2 θ range of 5°–80°. DLS measurements were done by using a Master-size2000 apparatus from Malvern Instruments. TG-DTA analyses were recorded using a Shimadzu apparatus in a Pt crucible. The heating rate was of 5° and 10 °C min⁻¹, respectively, starting from room temperature till 900 °C under a nitrogen flow of 10 mL min⁻¹. DRIFT spectra were recorded with a Thermo spectrometer 4700 (400 scans with a resolution of 4 cm⁻¹) in the range of 600–4000 cm⁻¹. CO₂- and NH₃-TPD measurements were carried out using the AutoChem II 2920 station. The samples (100–200 mg), placed in a U-shaped quartz reactor with an inner diameter of 0.5 cm, were pre-treated under He (Purity 5.0) at 80 °C for 1 h, and then exposed to a flow of CO₂ or a flow of 1 vol% NH₃ in helium, for 1 h. After that, the samples were purged with a flow of He (50 mL min⁻¹) for 20 min at 25 °C in order to remove the weakly adsorbed species. TPD was then started, with a heating rate of 10 °C min⁻¹ till 500 °C where was maintained for 30 min. The desorbed products were analyzed by GC-TCD chromatography. The desorbed CO₂/NH₃, expressed as mmoles of CO₂/NH₃ per gram of catalyst, was determined using a calibration curve. XPS measurements were performed at normal angle emission in a Specs setup, by using Al K α monochromated radiation ($h\nu = 1486.7$ eV) of an X-ray gun, operating at 300 W (12 kV/25 mA) power. A flood gun with electron acceleration at 1 eV and electron current of 100 μ A was used to avoid charge effects. Photoelectron energy was recorded in normal emission by using a Phoibos 150 analyzer, operating with pass energy of 30 eV. The XP spectra were fitted by using Voigt profiles combined with their primitive functions, for inelastic backgrounds. The Gaussian width of all lines and thresholds do not differ considerably from one spectrum to another, being always in the expected range of 2 eV. Scanning Electron Microscopy (SEM) analysis was carried out on a Hitachi S-4700 Cold Field Emission Gun Scanning Electron Microscope operating at an

acceleration voltage of 15 kV. Energy-dispersive X-ray spectroscopy (EDX) was performed for elemental analysis. Oxford EDS system was employed for these analyzes.

2.3. Catalytic tests

The activity tests were carried out in the batch mode as follows: 0.05 g of catalyst was added to a solution of 0.18 g (1.0 mmol) glucose in 5 mL water. After closing, the reactor was heated at 160–180 °C, under stirring (1000 rpm), for 6–12 h. Additional catalytic tests were made in the same conditions but in a biphasic solvent formed from 3.5 mL aqueous solution of 20 % NaCl and 1.5 mL organic solvent. 2-Sec-butylphenol (SBP), 2-tert-butylphenol (TBP) and methyl isobutyl ketone (MIBK) were used as organic solvents.

2.4. Catalytic recycling

After the first catalytic cycle the used catalyst was recovered by centrifugation, washed three times with water, and several times with water/methanol. The washed catalysts were dried at 80 °C for 48 h, and calcined at 450 °C for 4 h in a flow of N₂ (30 cm³.min⁻¹) prior to the next cycle.

2.5. Products analysis

After the reaction, the catalyst was separated by centrifugation and the reaction products were analysed in both phases by HPLC chromatography, in the following conditions: mobile phase: acetonitrile/water = 75/25; flow rate: 1 mL/min; detectors: diode-array detection (DAD), at 254 and 210 nm, and differential refractometer (RID); column: Zorbax Carbohydrate, 4.6 × 250 mm, 5 µm. Retention times: HMF: DAD, 254 nm: 2.86 min; RID: 3.09 min; levulinic acid: DAD, 210 nm: 7.6 min; RID: 7.9 min; fructose: DAD, 210 nm: 8.4 min; RID: 8.9 min; glucose: RID: 9.7 min, 10.1 min and 10.4 min.

3. Results and discussion

3.1. XRD characterization

Fig. 1 illustrates the XRD patterns of the two humins-derived catalysts, namely GHNb1.2 and GHNb1.7. The broad diffraction line at 15–30° is assigned to amorphous carbon composed of polycyclic aromatic carbon sheets oriented in a random manner [54]. After the deposition-precipitation of the niobium precursor a weak diffraction line

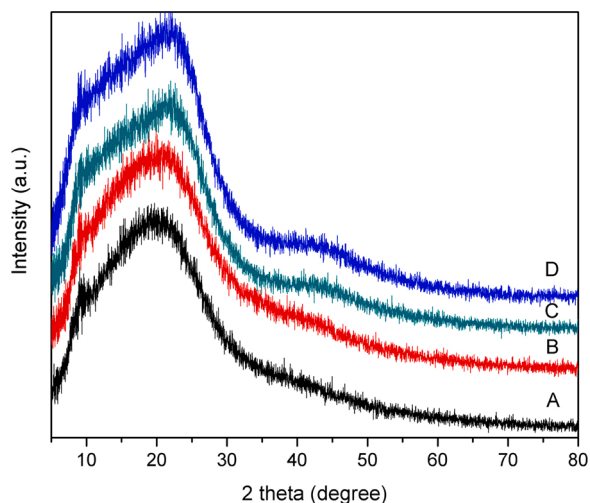


Fig. 1. XRD patterns of the humins and humins-derived Nb catalysts. A - humins; B -GHNb1.7 n.c. (non-calcined); C - GHNb1.7; D - GHNb1.2.

at 35–50° becomes visible, irrespective of the loading of niobia. Then, after calcination, the narrower diffraction line accompanied by a shift to higher 2θ corresponds to the formation of a graphite-like carbon structure that is also in concordance with previous reports [55]. No diffraction lines characteristic to niobia (ie, TT- [JCPDS card 00–028-0317] or T-phase [JCPDS card 00–030-0873]), were identified in these patterns suggesting either an amorphous phase of niobia or a high dispersion of the niobium oxide crystalline particles.

3.2. DLS measurements

DLS measurements confirmed changes in the size distribution of the catalysts as a function of the composition (Fig. 2). They also indicate that the presence of niobium induced a clearer bimodal size distribution of the dispersed particles that corresponds to the modification of the surface properties (wettability) by the impregnation-deposition conditions.

3.3. TG-DTA measurements

Thermogravimetric/differential (TG-DTA) thermal analyses of the humins support and catalytic samples showed an endothermic effect at around 50–60 °C that is associated to an weight loss assigned to physically adsorbing water (Figures S1) and a major weight loss of pristine humins (Figures S1) occurring as an exothermic effect, at 430 °C. This one can be attributed to different processes as dehydration, decarboxylation, and decarbonylation of humins resulting in the formation of a relative stable polycyclic aromatic structure that is also in accordance to previous literature reports [35,56]. Besides these, a third exothermic peak at 573 °C accompanying a further weight loss of pristine humins, can be associated to a further decomposition of oxygenated groups with the formation of a more stable carbon network (Figures S1).

The absence of any loss of mass for the GHNb1.2 and GHNb1.7 samples till 430 °C is the consequence of the calcination these samples. However, further heating of these samples led to a weight loss with an exothermic effect with a maximum at around 500 °C.

In conclusion, these measurements confirmed the thermal stability of the polycyclic aromatic structure at temperatures of 160–180 °C, ie under the reaction conditions and are in a good concordance to the XRD measurements.

3.4. SEM-EDS analysis

SEM images recorded on as-synthesized humins and calcined in nitrogen at 450 °C do not reveal strong alteration of the texture and morphology (Fig. 3). Spherical interconnected particles appear in agreement with previous observations [56].

SEM coupled with EDX analysis was performed on niobium-based samples. SEM images and elemental mapping are reported in Fig. 4 on GHNb1.7 sample before (GHNb1.7n.c.) and after calcination (GHNb1.7) and on calcined GHNb1.2. Similarly to previous observations, the presence of spherical particles still predominates emphasizing the fact that carburization during calcination in inert atmosphere should not occur significantly. Such assertion seems in rather good agreement with TG analysis which only shows significant weight loss above 430 °C. Nevertheless, in this temperature conditions elemental analysis clearly indicates a lower density of oxygen on calcined samples like due to the partial removal of oxygenates functionalities. Previous investigations pointed out possible rearrangement of the polymer network as well as aromatization of the structure.

Regarding the distribution of NbO_x species, it is worthwhile to note the absence of large and intense spots which could reflect the occurrence of strong aggregation process. As observed, niobium seems to be randomly distributed irrespective of the composition. Interestingly, some Nb-riched zones appear distinctly on GHNb1.7 which coincides with the spherical structures. Such observations are less pronounced on GHNb1.2 despite some heterogeneities are discernible. A questioning

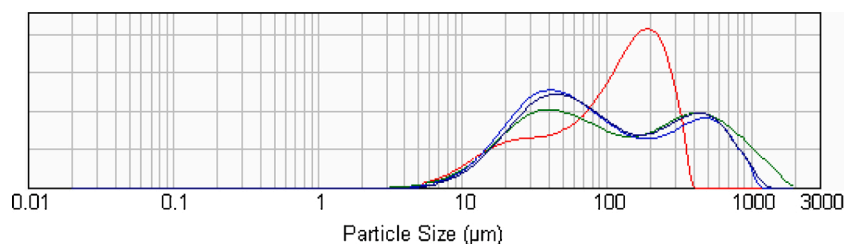


Fig. 2. Dispersed particle size distribution of the humins-based samples: humins (red), GHNb1.7n.c (black), GHNb1.2 (blue) and GHNb1.7 (green) (For interpretation of the references to colour in this figure legend, the reader is referred to the web version of this article.).

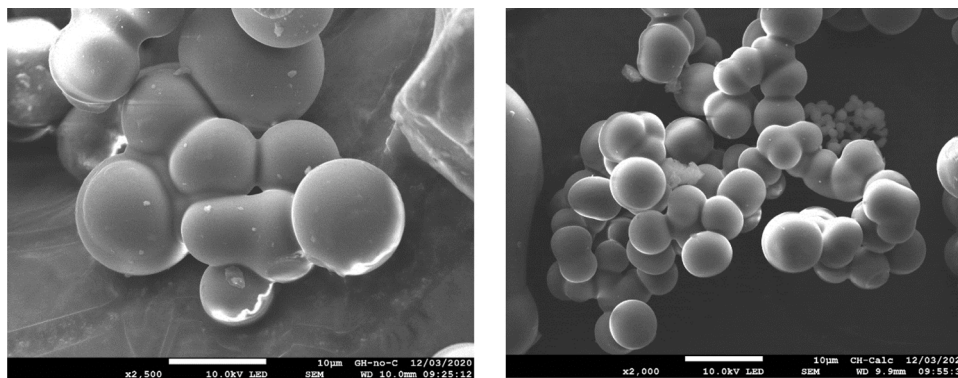


Fig. 3. SEM images recorded on as-synthesized humins (GH) and GH calcined in nitrogen at 450 °C.

point arise from these observations related to local formation of highly hydrophobic graphite-like carbon structure which could strengthen the interaction with oxidic Nb species.

3.5. DRIFT spectra

The DRIFT spectra of the humins and Nb-based samples are shown in Fig. 5. The DRIFT spectra of humins and GHNb1.7n.c. are very similar showing a broad band at around 3250 cm^{-1} , assigned to C—O stretching of alcohols groups, and a second one at around 2950 cm^{-1} , assigned to aliphatic C—H stretch (Fig. 5A). These bands are seen as shoulders due to the presence of the —OH groups. Differently, the spectra corresponding to calcined GHNb1.2 and GHNb1.7 show two additional bands at 3640 and 3059 cm^{-1} while the large band at 3250 cm^{-1} is narrower and shifted to 3323 cm^{-1} (Fig. 5A). These bands were attributed to —OH groups arisen from the presence of Nb(V)—OH species (3640 cm^{-1}) induced during the calcination step, and connected to the humins surface through C—OH groups. This also corresponds to diminution of the population of the humins surface —OH groups (3250 cm^{-1}). However, irrespective of the Nb-based sample, no additional bands at $3555\text{--}3602\text{ cm}^{-1}$ were observed, confirming the absence of Nb (IV) species in these materials.

In the $1800\text{--}400\text{ cm}^{-1}$ range (Fig. 5B) the recorded spectra display the C=O stretching (1700 cm^{-1}) resulting from the presence of acid, aldehyde, and ketone groups, conjugated with C=C ascribed to substituted furan rings. Then, the band at 1600 cm^{-1} can be assigned to a C=C stretch, while the band at 1025 cm^{-1} to a C—O stretch of the furan ring deformation [27]. Bands at around 800 and 765 cm^{-1} are characteristic to the C—H out-of-plane deformation and to substituted furans [11,27].

The DRIFT spectra of GHNb1.2 and GHNb1.7 showed, in addition to the bands recorded for of the humins (however with major differences in the relative intensities (Fig. 5B)) new bands located at 1700 cm^{-1} (assigned to C=O stretching conjugated with C=O) and 1440 and 873 cm^{-1} (assigned to stretching vibration of the C=C and the presence of the niobyl Nb=O species [57]). The intensification of the band at

765 cm^{-1} , characteristic to substituted furans, and that at 800 cm^{-1} accompanied by a small shift at 813 cm^{-1} , indicates both structural modifications of the pristine humins towards a more polyaromatic structure.

3.6. XPS analysis

The XPS analysis is reflected by deconvoluted spectra (Figures S2-S5) and binding energies listed in Table S1. Thus, the deconvoluted spectra of the C1s level led to components assigned to C1s-sp² hybridized C (C=C, $284.5\text{--}284.6\text{ eV}$), hydroxyl/epoxy/ether (C—OH/C—O—C, $285.5\text{--}285.9\text{ eV}$), carbonyl (C=O, $286.7\text{--}287.2\text{ eV}$), and carboxyl (HO—C=O, 288.9 eV) functionalities. Deconvolution of the O1s level corresponded to carboxyl (HO—C=O, $530.2\text{--}531.2\text{ eV}$), carbonyl (C=O, $531.7\text{--}532.2\text{ eV}$), hydroxyl (C—OH, $532.7\text{--}533.4\text{ eV}$) and epoxy/ether (C—O—C, $533.7\text{--}534.6\text{ eV}$) functionalities [58]. The binding energy of the Nb 3d_{5/2} level ($207.0\text{--}207.1\text{ eV}$) corresponded to Nb(V) species (Figures S3-S5 and Table S1). Table 1 presents the surface XPS composition of investigated catalysts. It indicates a decrease in the surface oxygen after the calcination step that also paralleled a slight increase in the surface niobium. Interesting enough, the concentration of surface niobium is quite similar for samples prepared from different loadings of the niobium and with a different analytic content (ie 0.03 and 0.04 mol\%Nb for GHNb1.2 and GHNb1.7, respectively). Also, the XPS affirmed the presence of the Nb(IV) species that is also in agreement with the DRIFT analysis. However, the SEM analysis suggests a somehow different distribution on the surface of the calcined catalyst. For GHNb1.2, niobium is merely homogeneously (Fig. 4C) distributed while for the GHNb1.7 some Nb-riched areas were detected (Fig. 4B). No any large niobium oxide aggregate was detected.

3.7. CO₂- and NH₃-TPD measurements

CO₂- and NH₃-TPD analyses revealed the acid-base properties of both pristine humins and GHNb samples confirming the presence of both acid and basic sites but with a different relative population (Table 2) that

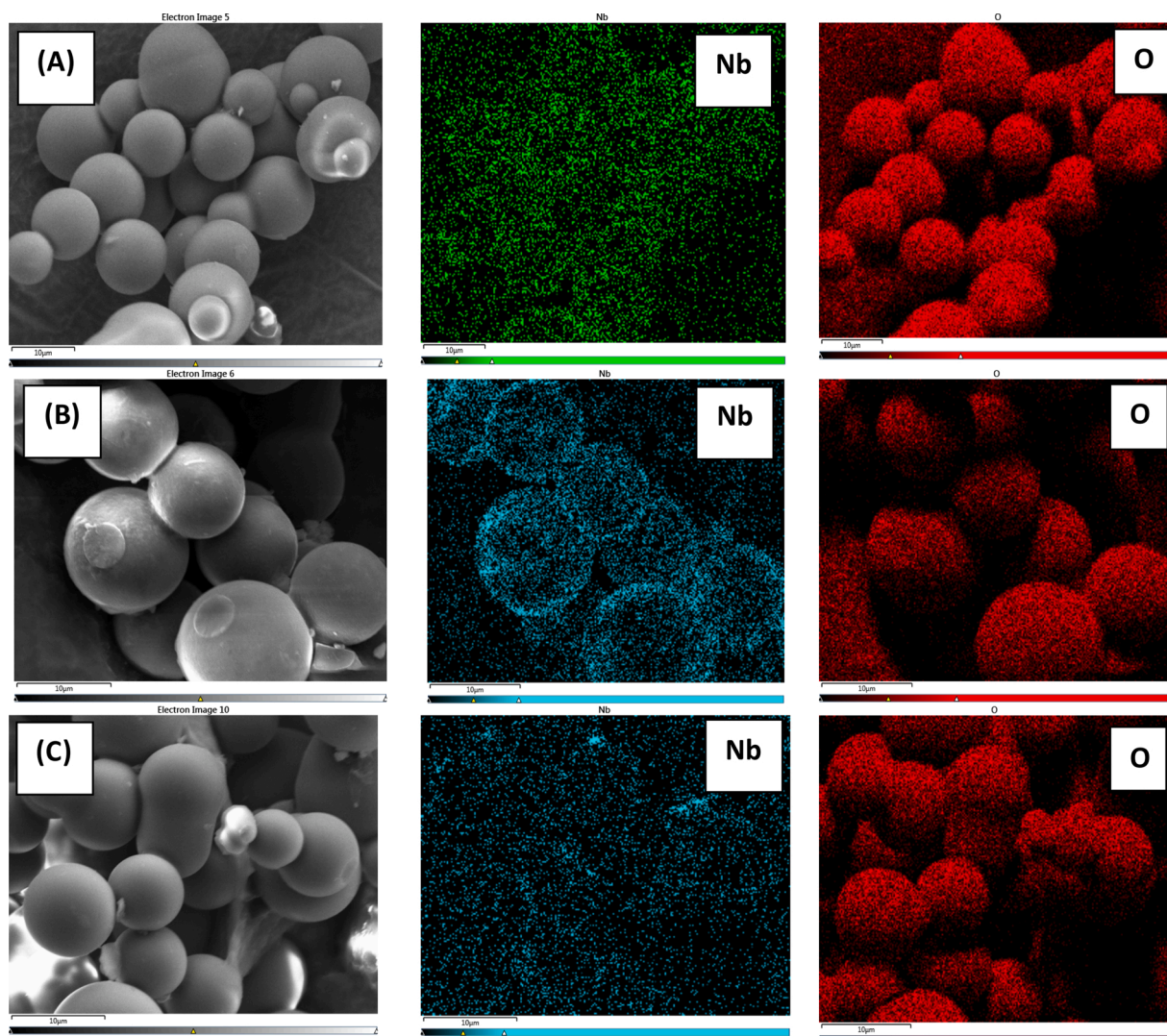


Fig. 4. SEM images and elemental analysis recorded on GHNb1.7n.c. (A), GHNb1.7 (B) and on calcined GHNb1.2 (C).

depends on both the presence of niobium and the calcination conditions. Thus, the humins impregnation with the niobium precursor in the presence of urea led to an increased concentration of the base sites while the pristine concentration of acid sites remains constant (ie, GHNb1.7n.c. sample, entry 2). The calcination results in a high decreases of the acid sites concentration while the total concentration of base sites remained apparently un-affected (ie, GHNb1.7n.c., entry 2 *versus* GHNb1.7, entry 4). However, the nature of the base sites in the calcined sample seems to be different by comparison with those existing in the pristine humins. These new stronger base sites may originate from the ammonium niobate (V) oxalate hydrate complex impregnation/deposition step but also from the —OH groups arisen from the Nb(V)—OH species, in accordance to the DRIFT results. The acidity can be generated by different species, such as the Nb=O , $\text{NbO-H}_{(\text{acid})}$ or organic acid groups still existent on the carrier surface.

For the final catalysts the base/acid sites ratio increased from 1.76 (GHNb1.2) to 4.25 (GHNb1.7), which may corresponds to the formation of Nb-riched zones for the last sample.

3.8. Catalytic behavior of Nb-based humins catalysts

The valorization of humins as materials, including catalysts, is still at the proof-of-principle stage. Their structure is still incomplete understood and, as a specific example, a limited number of characterization

studies have been reported for humins prepared from monomeric sugars. These indicate that pristine humins possess a furan-rich structure with ether and (hemi) acetal linkages [59]. However, under basic conditions, as those utilized for the impregnation-deposition of niobium species, an arene-rich structure could be generate at the expense of the furan content [24]. Finally, after calcination of niobium deposited onto humins supplementary structural modifications may undergo toward the formation of a graphite-like carbon structure, as XRD demonstrated in this study. This can also be accompanied by the formation of novel base sites onto the humins surface leading to catalysts presenting acid-base bi-functionality.

In this study, the catalytic behavior of the niobia/humins catalysts was investigated in the one-pot conversion of the glucose to HMF in a biphasic system consisting of a combination of glucose dehydration under aqueous conditions and an *in situ* extraction of the HMF in an organic phase [18,44,60,61]. With this purpose, different phases as methyl-isobutyl-ketone (MIBK), 2-tert-butylphenol (TBP) and 2-sec-butylphenol (SBP) were used as an extraction solvent. Previously work conducted in our group, showed that highly dispersed Nb species into a zeolite matrix [47] display a high catalytic efficiency in glucose dehydration to HMF (selectivities to MHF of 84.3 %, for a conversion of glucose of 97.4 %, at 180 °C and after 12 h) in a biphasic water/MIBK solvent [18]. However, other reports indicate 2-sec-butylphenol (SBP) as an efficient extraction solvent, its advantage being generate by higher

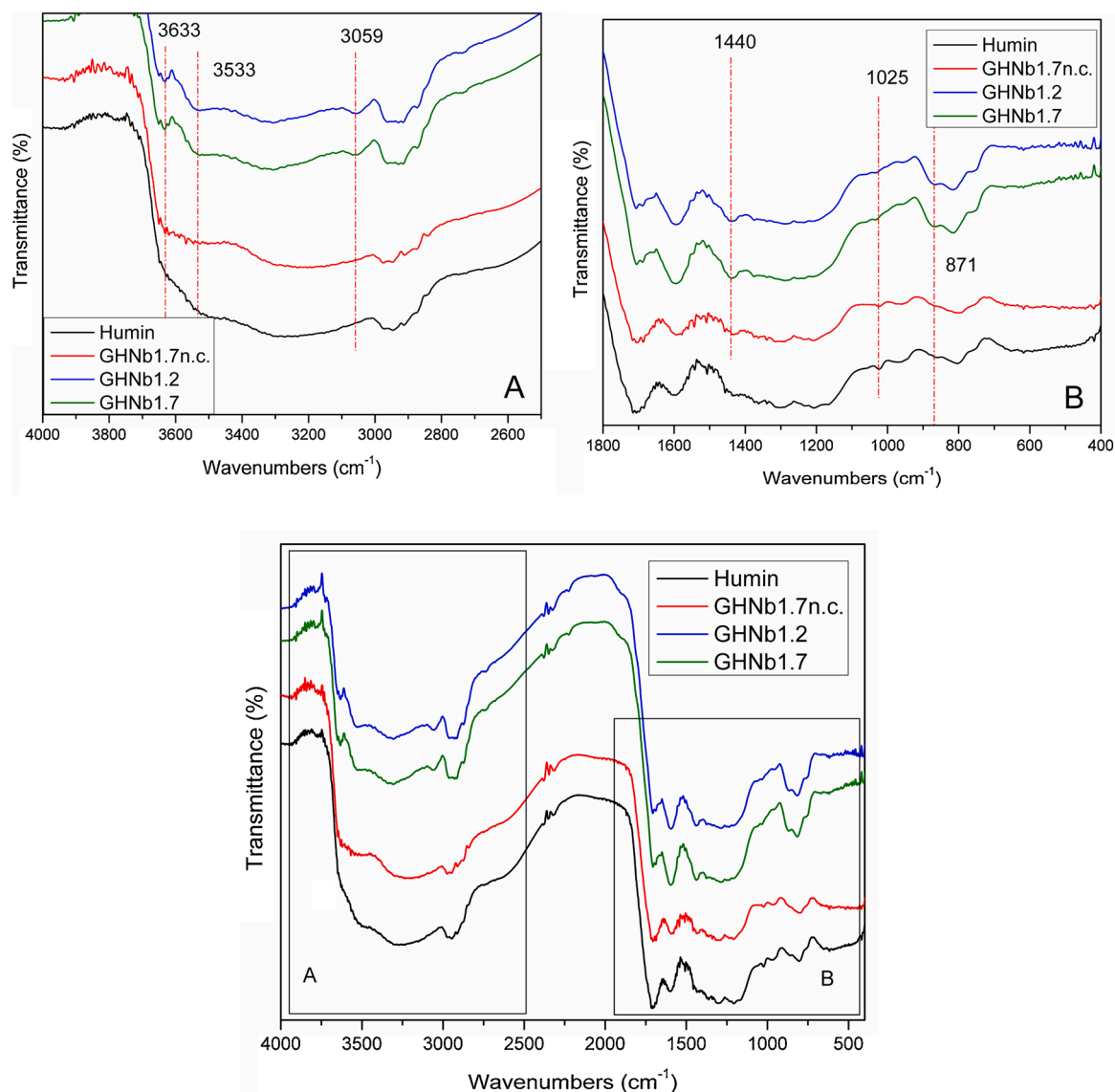


Fig. 5. DRIFT spectra of humins (black), GHNb1.7n.c. (red), GHNb1.7 (green) and GHNb1.2 (blue) samples. Ranges of 4000–2500 cm^{-1} and 1800–400 cm^{-1} are magnified in (A) and (B) figures (For interpretation of the references to colour in this figure legend, the reader is referred to the web version of this article.).

Table 1
Surface XPS composition of investigated samples.

Samples	C, at %	O, % at	Nb, % at	O/C	Nb/O
Humins	81.4	18.6	–	0.23	–
GHNb1.7 n.c.	78.8	19.3	1.9	0.24	0.10
GHNb1.2	81.7	16.0	2.4	0.20	0.15
GHNb1.7	81.4	16.3	2.3	0.20	0.14

Table 2
Acid-base sites concentration determined through NH_3 - and CO_2 -TPD.

Entry	Sample	Acid sites concentration (mmols $\text{NH}_3/\text{g}_{\text{cat}}$) < 100 °C	Base sites concentration (mmols $\text{CO}_2/\text{g}_{\text{cat}}$)			Base/acid ratio
			<100 °C	> 150 °C	Total	
1	Humins	0.042	0.022	0.0004	0.0224	0.53
2	GHNb1.7 n.c.	0.042	0.049	0.033	0.0820	1.95
3	GHNb1.2	0.021	0.021	0.016	0.0370	1.76
4	GHNb1.7	0.020	0.028	0.057	0.0850	4.25

HMF yields compared to other organic solvents such as tetrahydrofuran (THF), methyl isobutyl ketone (MIBK), and 2-butanol [62,63].

In this study, results collected from a series of catalytic experiments highlighted some very important features. Reactions carried out at 140–180 °C for 6–12 h led to the very good yield to HMF, with a maximum for a temperature of 180 °C and a reaction time of 8 h, irrespective of the extracting solvent (ie, MIBK, TBP and SBP) or the catalyst nature. However, the presence of NaCl in the aqueous phase induces an important difference between an inefficient and a highly efficient catalytic system (Table 3).

As Table 3 shows, in the presence of the calcined humins no HMF was detected into reaction products (entry 1, Table 3) that might be attributed to the graphite-like carbon structure of calcined humins with a low concentration of weak surface acid/base functional groups. The HMF production in pure water or TBP, as monophasic solvent, is also not a viable option for the HMF synthesis (GHNb1.2 catalyst, in monophasic solvent, entries 2 and 3, Table 3), presumably due to the slow rate of HMF formation and fast rehydration to furan ring opening products, such as levulinic acid (LA) and formic acid [64,65].

Replacing the monophasic solvent with a bi-phasic TBP/water, the HMF starts to accumulate (entry 4, Table 3) and a yield of 16 % HMF was

Table 3
Catalytic results in glucose dehydration to HMF in biphasic systems.

Entry	Catalyst	Solvent	Yield HMF, (%)
1	Calcined GH	TBP/water	0
2	GHNb1.2	Water	0
3	GHNb1.2	TBP	0
4 ^a	GHNb1.2	TBP/water	16
5	GHNb1.2	TBP/water	96
6	GHNb1.2	SBP/water	38
7	GHNb1.2	MIBK/water	15
8	GHNb1.7	TBP/water	85
9	GHNb1.7	SBP/water	24
10	GHNb1.7	MIBK/water	14

Reaction conditions: glucose 0.18 g (1 mmol), 50 mg of catalyst, solvent [3.5 mL H₂O (NaCl 20 %) +1.5 mL extracting solvent], reaction temperature: 180 °C, reaction time: 8 h, 1000 rpm.

^a No NaCl in aqueous phase.

determined in reaction products. However, as already reported [66], the presence of NaCl in the aqueous phase plays an important role in improving the partition coefficient of HMF. Indeed, in bi-phasic TBP/water system and 20 %NaCl in the aqueous phase, the yield to HMF highly increased from 16 % to 96 % (entry 5, Table 3).

The nature of the catalysts and organic solvents plays an important role in determining an effective extraction of HMF. Using the same approach, ie a biphasic system consisting of methyl-isobutyl-ketone (MIBK) as extraction solvent and aqueous NaCl (20 %) salt, Nb-based humins catalysts produced HMF in much lower yields (15 %, on GHNb1.2 catalyst) than previously reported Nb-based Beta zeolite catalysts (82.1 % at 180 °C and 12 h) [18]. Moreover, these catalysts have different degrees of hydrophilicity. Accordingly, the Nb-based Beta zeolite catalyst was located in the aqueous phase while the GHNb1.2 one was located in the organic phase indicating its high hydrophobicity. Such a behavior led to significant differences in the glucose conversion to HMF. This statement is also supported by the work of Datye and co-workers [53] which showed that different applied preparation methodologies lead to Nb-based carbonous carriers with different degrees of hydrophilicity, and hence with different locations in the biphasic water/SBP system. According with this location their catalytic behavior in the conversion of glucose to HMF was highly affected. A comparison of the obtained results in this work with those reported by Datye and co-workers [53], in similar biphasic systems, indicates the superiority of our developed materials in terms of HMF yields. Clearly enough, the differences highly depend on both the location of the catalyst and the intrinsic catalytic features.

However, by changing the extraction solvent from MIBK to SBP, in the presence of GHNb1.2 catalyst and under similar reaction conditions, the yield in HMF increased to 57 %, after only 8 h (entry 6, Table 3). The different reaction results are supported by the value of the partition coefficient which highly increases for all organic solvents in the presence of NaCl. However, its relative increase depends on the nature of the organic solvent and is explained by a salting-out effect [67,68].

Working under the same experimental conditions in the presence of the GHNb1.7 the trend was similar but the yields were smaller than those obtained in the presence of the GHNb1.2 (entries 8–10, Table 3). With GHNb1.7 the highest yield to HMF (85 %) was obtained in bi-phasic TBP/water and 20 %NaCl in the aqueous phase, while in bi-phasic SBP/water system and 20 %NaCl in the aqueous phase, the yield to HMF reached only 24 %. These results confirm the importance of the base/acid ratio in this reaction. As XPS measurements showed, the concentration of superficial niobium is similar in both GHNb1.2 and GHNb1.7 catalysts but the TPD measurements evidenced a much higher base/acid sites ratio in the GHNb1.7 one (4.25). However, GHNb1.7 led to lower yields to HMF. A high yield to HMF requires an optimum base/acid sites ratio and as it has been demonstrated this condition is fulfilled for GHNb1.2 with a ratio of 1.76.

In the second catalytic cycle the initial yield to HMF decreased until < 60 % (for GHNb1.2 catalyst, reaction conditions similar to entry 5, Table 3). This high decreases may be due to the structural modifications of the carbonous carrier as an effect of the methanol washing solvent. In agree with literature [69], adopting different washing solvent in the humins-based catalysts recycle might result in the different recycling performances, as the solubilities of the polycyclic aromatic hydrocarbons in the different washing solvents are varied. Further study about the effect of washing solvent on the stability will be conducted in our following work.

4. Conclusions

In summary, in this paper we report a novel active and selective catalyst for the one-pot catalytic transformation of glucose to HMF, prepared by the deposition precipitation-carbonization (DPC) of ammonium niobate(V) oxalate hydrate over humins carrier produced by glucose dehydration. After calcination resulted catalysts with highly dispersed niobia particles anchored onto the graphite-like carbon carrier. This preparation procedure afforded an unexpected highly efficient catalyst for the HMF synthesis. The distribution of niobium species on the carrier surface makes the difference between an efficient and an less-efficient catalyst. Thus, for the same concentration of surface niobium (ie, 2.4at% from XPS analysis) deposited on, a relatively more homogeneous distribution (SEM analysis) as —Nb—OH and Nb=O species (DRIFT analysis) leads to an efficient catalyst while the agglomeration in relatively rich areas determines an appreciable decrease of the HMF yield. The relative base/acid sites ratio is influenced by the distribution of niobium, the formation of Nb-rich particles corresponding to an increased ratio.

The highest yield to HMF (96 %) was obtained with the GHNb1.2 (0.03 mol% Nb) catalyst in a bi-phasic TBP/water system, at 180 °C after 8 h.

In conclusion, these results confirm that by-products of renewable biomass-based technologies, such as humins, may offer valuable solutions for the production of important chemicals, such as HMF and, in this way, to provide support for a sustainable economy.

CRedit authorship contribution statement

Magdi El Fergani: Methodology, investigation, validation of the catalysts synthesis and catalytic tests. **Natalia Candu:** Investigation and validation of part of catalysts characterization techniques. **Madalina Tudorache:** Investigation and validation of the reaction products identification and analysis. **Cristina Bucur:** Investigation and validation of XPS measurements. **Nora Djelal:** Investigation and validation of SEM-EDX measurements. **Pascal Granger:** Coordination for part of the catalysts preparation and characterization research activity planning and execution, writing-reviewing and editing, funding acquisition. **Simona M. Coman:** Conceptualization, coordination for the research activity planning and execution, writing original draft preparation, writing-reviewing and editing, funding acquisition.

Declaration of Competing Interest

The authors report no declarations of interest.

Acknowledgements

Simona M. Coman kindly acknowledges UEFISCDI for the financial support (project PN-III-P4-ID-PCE-2016-0533, Nr. 116/2017). Magdi El Fergani kindly acknowledges ERASMUS and the PICS “Nanocat” N°230460 for supporting and partially funding this work.

Appendix A. Supplementary data

Supplementary material related to this article can be found, in the online version, at doi:<https://doi.org/10.1016/j.apcata.2021.118130>.

References

- [1] K. Triantafyllidis, A. Lappas, M. Stöcker, *The Role of Catalysis for the Sustainable Production of Bio-fuels and Bio-chemicals*, Elsevier Ltd., Oxford, UK, 2013. ISBN: 978-0-444-56330-56339.
- [2] R. Luque, A.M. Balu, *Producing Fuels and Fine Chemicals from Biomass using Nanomaterials*, CRC Press, Taylor & Francis Group, Boca Raton, 2014. ISBN (PDF): 978-1-4665-5340-5348.
- [3] V. Blay, L.F. Bobadilla, A. Cabrera-Garcia, *Zeolites and Metal-Organic Frameworks: From Lab to Industry*, Amsterdam University Press, 2018. ISBN: 978-94-6298-556-558.
- [4] A. Balu, A.G. Nunez, *Biomass and Biowastes – New Chemical Products From Old*, De Gruyter GmbH Publisher, 2020. ISBN-10: 3110537788; ISBN-13: 978-3110537789.
- [5] R. Mariscal, P. Maireles-Torres, M. Ojeda, I. Sádaba, M. López Granados, *Energy Environ. Sci.* 9 (4) (2016) 1144–1189, <https://doi.org/10.1039/C5EE02666K>.
- [6] F.D. Pileidis, M.M. Titirici, *Chem. Sus. Chem.* 9 (6) (2016) 562–582, <https://doi.org/10.1002/cssc.201501405>.
- [7] P. Sudarsanam, R. Zhong, S.V.d. Bosch, S.M. Coman, V.I. Parvulescu, B.F. Sels, *Chem. Soc. Rev.* 47 (2018) 8349–8402, <https://doi.org/10.1039/C8CS00410B>.
- [8] J.J. Bozell, G.R. Petersen, *Green Chem.* 12 (2010) 539–554, <https://doi.org/10.1039/B922014C>.
- [9] B.F.M. Kuster, H.S.V.D.Baan van der Baan, *Carbohydr. Res.* 54 (2) (1977) 165–176, [https://doi.org/10.1016/S0008-6215\(00\)84806-5](https://doi.org/10.1016/S0008-6215(00)84806-5).
- [10] R. Weingarten, J. Cho, R. Xing, W.C. Conner, G.W. Huber, *Chem. Sus. Chem.* 5 (2012) 1280–1290, <https://doi.org/10.1002/cssc.201100717>.
- [11] S.K.R. Patil, J. Heltzel, C.R.F. Lund, *Energy Fuels* 26 (8) (2012) 5281–5293, <https://doi.org/10.1021/ef3007454>.
- [12] D.M. Alonso, S.G. Wettstein, J.Q. Bond, T.W. Root, J.A. Dumesic, *Chem. Sus. Chem.* 4 (2011) 1078–1081, <https://doi.org/10.1002/cssc.201100256>.
- [13] H. Zhao, J.E. Holladay, H. Brown, Z.C. Zhang, *Science* 316 (2007) 1597–1600, <https://doi.org/10.1126/science.1141199>.
- [14] C. Fan, H. Guan, H. Zhang, J. Wang, S. Wang, X. Wang, *Biomass Bioenerg.* 35 (2011) 2659–2665, <https://doi.org/10.1016/j.biombioe.2011.03.004>.
- [15] H. Yan, Y. Yang, D. Tong, X. Xiang, C. Hu, *Catal. Commun.* 10 (2009) 1558–1563, <https://doi.org/10.1016/j.catcom.2009.04.020>.
- [16] F. Yang, Q. Liu, X. Bai, Y. Du, *Bioresour. Technol. Rep.* 102 (2011) 3424–3429, <https://doi.org/10.1016/j.biortech.2010.10.023>.
- [17] L. Hu, G. Zhao, W. Hao, X. Tang, Y. Sun, L. Lin, S. Liu, *RSC Adv.* 2 (2012) 11184–11206, <https://doi.org/10.1039/C2RA21811A>.
- [18] N. Candu, M. El Fergani, M. Verziu, B. Cojocaru, B. Jurca, N. Apostol, C. Teodorescu, V.I. Parvulescu, S.M. Coman, *Catal. Today* 325 (2019) 109–116, <https://doi.org/10.1016/j.cattod.2018.08.004>.
- [19] G. Yang, E.A. Pidko, E.J.M. Hensen, *J. Catal.* 295 (2012) 122–132, <https://doi.org/10.1016/j.jcat.2012.08.002>.
- [20] T.M.C. Hoang, E.R.H.V. Eck, W.P. Bula, J.G.E. Gardeniers, L. Lefferts, K. Seshan, *Green Chem.* 17 (2015) 959–972, <https://doi.org/10.1039/C4GC01324G>.
- [21] M. Sevilla, A.B. Fuertes, *Carbon* 47 (2009) 2281–2289, <https://doi.org/10.1016/j.carbon.2009.04.026>.
- [22] M. Sevilla, A.B. Fuertes, *Chem. Eur. J.* 15 (2009) 4195–4203, <https://doi.org/10.1002/chem.200802097>.
- [23] C. Yao, Y. Shin, L.Q. Wang, C.F. Windisch, W.D. Samuels, B.W. Arey, C. Wang, W. M. Risen, G.J. Exarhos, *J. Phys. Chem. C* 111 (42) (2007) 15141–15145, <https://doi.org/10.1021/jp0741881>.
- [24] I.V. Zandvoort, E.J. Koers, M. Weingarth, P.C. Bruijninx, M. Baldus, B. M. Weckhuysen, *Green Chem.* 17 (2015) 4383–4392, <https://doi.org/10.1039/C5GC00327J>.
- [25] T.M.C. Hoang, L. Lefferts, K. Seshan, *Chem. Sus. Chem.* 6 (2013) 1651–1658, <https://doi.org/10.1002/cssc.201300446>.
- [26] S.K. Patil, C.R. Lund, *Energy Fuels* 25 (2011) 4745–4755, <https://doi.org/10.1021/ef2010157>.
- [27] I.V. Zandvoort, Y. Wang, C.B. Rasrendra, E.R.V. Eck, P.C. Bruijninx, H.J. Heeres, B.M. Weckhuysen, *Chem. Sus. Chem.* 6 (2013) 1745–1758, <https://doi.org/10.1002/cssc.201300332>.
- [28] G. Tsilomelekis, M.J. Orella, Z. Lin, Z. Cheng, W. Zheng, V. Nikolakis, D.G. Vlachos, *Green Chem.* 18 (2016) 1983–1993, <https://doi.org/10.1039/C5GC01938A>.
- [29] I.V. Zandvoort, Y. Wang, C.B. Rasrendra, E.R.H.V. Eck, P.C.A. Bruijninx, H. J. Heeres, B.M. Weckhuysen, *Chem. Sus. Chem.* 6 (9) (2013) 1745–1758, <https://doi.org/10.1002/cssc.201300332>.
- [30] N. Baccile, G. Laurent, F. Babonneau, F. Fayon, M.M. Titirici, M. Antonietti, *J. Phys. Chem. C* 113 (2009) 9644–9654, <https://doi.org/10.1021/jp901582x>.
- [31] Y.Z. Mi, W.B. Hu, Y.M. Dan, Y.L. Liu, *Mater. Lett.* 62 (2008) 1194–1196, <https://doi.org/10.1016/j.matlet.2007.08.011>.
- [32] Y. Wang, S. Agarwal, A. Kloekhorst, H.J. Heeres, *Chem. Sus. Chem.* 9 (9) (2016) 951–961, <https://doi.org/10.1002/cssc.201501371>.
- [33] S. Agarwal, Dv. Es, H.J. Heeres, *J. Anal. Appl. Pyrol.* 123 (2017) 134–143, <https://doi.org/10.1016/j.jaap.2016.12.014>.
- [34] J.M. Pin, N. Guigo, A. Mija, L. Vincent, N. Sbirrazzuoli, J.C.V.D. Waal, E.D. Jong, *ACS Sustain. Chem. Eng.* 2 (9) (2014) 2182–2190, <https://doi.org/10.1021/sc5003769>.
- [35] A. MijaJan, J.C.V.D. Waal, J.M. Pin, N. Guigo, E.D. Jong, *Constr. Build. Mater.* 139 (2017) 594–601, <https://doi.org/10.1016/j.conbuildmat.2016.11.019>.
- [36] D.J. Hayes, J. Ross, M.H.B. Hayes, S.W. Fitzpatrick, in: B. Kamm, P.R. Gruber, M. Kamm (Eds.), *Biorefineries - Industrial Processes and Products*, Wiley, Germany, 2006, pp. 139–164.
- [37] Z. Liu, F.S. Zhang, *J. Hazard. Mater.* 167 (2009) 933–939, <https://doi.org/10.1016/j.jhazmat.2009.01.085>.
- [38] P. Regmi, J.L. Garcia Moscoso, S. Kumar, X. Cao, J. Mao, G. Schafran, *J. Environ. Manag.* 109 (2012) 61–69, <https://doi.org/10.1016/j.jenvman.2012.04.047>.
- [39] M. Okamura, A. Takagaki, M. Toda, J.N. Kondo, K. Domen, T. Tatsumi, M. Hara, S. Hayashi, *Chem. Mater.* 18 (13) (2006) 3039–3045, <https://doi.org/10.1021/cm0605623>.
- [40] S. Suganuma, K. Nakajima, M. Kitano, D. Yamaguchi, H. Kato, S. Hayashi, M. Hara, *J. Am. Chem. Soc.* 130 (38) (2008) 12787–12793, <https://doi.org/10.1021/ja803983h>.
- [41] X. Qi, H. Guo, L. Li, R.L. Smith, *Chem. Sus. Chem.* 5 (11) (2012) 2215–2220, <https://doi.org/10.1002/cssc.201200363>.
- [42] J. Yang, G. Li, L. Zhang, S. Zhang, *Catalysts* 8 (1) (2018) 14, <https://doi.org/10.3390/catal8010014>.
- [43] L. Filicciotto, A.M. Balu, A.A. Romero, E.R. Castellón, J.C.V.D. Waal, R. Luque, *Green Chem.* 19 (18) (2017) 4423–4434, <https://doi.org/10.1039/C7GC01405H>.
- [44] R.J.V. Putten, J.C.V.D. Waal, E.D. Jong, C.B. Rasrendra, H.J. Heeres, J.G.D. Vries, *Chem. Rev.* 113 (2013) 1499–1597, <https://doi.org/10.1021/cr300182k>.
- [45] R. Otomo, T. Yokoi, J.N. Kondo, T. Tatsumi, *Appl. Catal. A Gen.* 470 (2014) 318–326, <https://doi.org/10.1016/j.apcata.2013.11.012>.
- [46] K. Nakajima, Y. Baba, R. Noma, M. Kitano, J.N. Kondo, S. Hayashi, M. Hara, *J. Am. Chem. Soc.* 133 (2011) 4224–4227, <https://doi.org/10.1021/ja110482r>.
- [47] M. El Fergani, N. Candu, S.M. Coman, V.I. Parvulescu, *Molecules* 22 (12) (2017) 2218, <https://doi.org/10.3390/molecules22122218>.
- [48] Q. Yang, M. Sherbath, T. Runge, *ACS Sustainable Chem. Eng.* 4 (2016) 3526–3534, <https://doi.org/10.1021/acssuschemeng.6b00587>.
- [49] C. Liu, J.M. Carraher, J.L. Swedberg, C.R. Herndon, C.N. Fleitman, J.P. Tessonnier, *ACS Catal.* 4 (2014) 4295–4298, <https://doi.org/10.1021/cs501197w>.
- [50] S. Lima, A.S. Dias, Z. Lin, P. Brandao, P. Ferreira, M. Pillinger, J. Rocha, V. C. Casilda, A.A. Valente, *Appl. Catal. A Gen.* 339 (2008) 21–27, <https://doi.org/10.1016/j.apcata.2007.12.030>.
- [51] P. Zhou, Z.H. Zhang, *Catal. Sci. Technol.* 6 (2016) 3694–3712, <https://doi.org/10.1039/C6CY00384B>.
- [52] H.F. Xiong, H.N. Pham, A.K. Datye, *J. Catal.* 302 (2013) 93–100, <https://doi.org/10.1016/j.jcat.2013.03.007>.
- [53] H. Xiong, T. Wang, B.H. Shanks, A.K. Datye, *Catal. Lett.* 143 (2013) 509–516, <https://doi.org/10.1007/s10562-013-1004-8>.
- [54] J. Yang, H. Zhang, Z. Ao, S. Zhang, *Catal. Commun.* 123 (2019) 109–113, <https://doi.org/10.1016/j.catcom.2019.02.016>.
- [55] W.Y. Lou, Q. Guo, W.J. Chen, M.H. Zong, H. Wu, T.J. Smith, *Chem. Sus. Chem.* 5 (8) (2012) 1533–1541, <https://doi.org/10.1002/cssc.201100811>.
- [56] J. Yang, X. Niu, H. Wub, H. Zhang, Z. Ao, S. Zhang, *Waste Manage.* 103 (2020) 407–415, <https://doi.org/10.1016/j.wasman.2020.01.004>.
- [57] F.F.P. Medeiros, M.F.V. Moura, A.G.P. da Silva, C.P. Souza, K.K.P. Gomes, U. Gomes, *Brazilian J. of Chem. Eng.* 23 (2006) 531–538, <https://www.scielo.br/pdf/bjce/v23n4/11.pdf>.
- [58] R. Al-Gaashania, A. Najjar, Y. Zakaria, S. Mansour, M.A. Atieh, *Ceram. Int.* 45 (2019) 14439–14448, <https://doi.org/10.1016/j.ceramint.2019.04.165>.
- [59] I.V. Sumerskii, S.M. Krutov, M.Y. Zarubin, *Russ. J. Appl. Chem.* 83 (2010) 320–327, <https://doi.org/10.1134/S1070427210020266>.
- [60] M.M. Recio, I.J. Morales, P.L. Arias, J.S. González, P.M. Torres, *ChemistrySelect.* 2 (2017) 2444–2451, <https://doi.org/10.1002/slct.201700097>.
- [61] E. Nikolla, Y. Román-Leshkov, M. Moliner, M.E. Davis, *ACS Catal.* 1 (2011) 408–410, <https://doi.org/10.1021/cs2000544>.
- [62] Y.J.P. Torres, T. Wang, J.M.R. Gallo, B.H. Shanks, J.A. Dumesic, *ACS Catal.* 2 (2012) 930–934, <https://doi.org/10.1021/cs300192z>.
- [63] Y.R. Leshkov, J.A. Dumesic, *Top. Catal.* 52 (2009) 297–303, <https://doi.org/10.1007/s11244-008-9166-0>.
- [64] X. Qi, M. Watanabe, T.M. Aida, R.L. Smith, *Green Chem.* 11 (2009) 1327–1331, <https://doi.org/10.1039/B905975J>.
- [65] F.S. Asghari, H. Yoshida, *Ind. Eng. Chem. Res.* 46 (2007) 7703–7710, <https://doi.org/10.1021/ie061673e>.
- [66] B. Saha, M.M.A. Omar, *Green Chem.* 16 (2014) 24–38, <https://doi.org/10.1039/C3GC41324A>.
- [67] E.O. Eisen, J. Joffe, *J. Chem. Eng. Data* 11 (1966) 480–484, <https://doi.org/10.1021/je60031a007>.
- [68] T.C. Tan, S. Aravinth, *Fluid Phase Equilib.* 163 (1999) 243–257, [https://doi.org/10.1016/S0378-3812\(99\)00231-9](https://doi.org/10.1016/S0378-3812(99)00231-9).
- [69] J. Yang, X. Niu, H. Wub, H. Zhang, Z. Ao, S. Zhang, *Waste Manag.* 103 (2020) 407–415, <https://doi.org/10.1016/j.wasman.2020.01.004>.